Hindawi
Scientific Programming
Volume 2021, Article ID 7007169, 7 pages
https://doi.org/10.1155/2021/7007169

Research Article

IMRT Images Based on Swarm Intelligence Algorithm in the Treatment of Nasopharyngeal Carcinoma and Pain

Xiaoli Fu,[1] **Minxiang Li**,[2] **Mantian Yin**,[3] **Qing Li**,[3] **and Ying Chen**[3]

[1]*Department of Urology, Second Affiliated Hospital of Hainan Medical College, Haikou 570311, China*
[2]*Department of Nursing, Second Affiliated Hospital of Hainan Medical College, Haikou 570311, China*
[3]*Department of Oncology, Second Affiliated Hospital of Hainan Medical College, Haikou 570311, China*

Correspondence should be addressed to Minxiang Li; 2620130006@stu.cpu.edu.cn

Received 14 May 2021; Accepted 13 July 2021; Published 27 July 2021

Academic Editor: Gustavo Ramirez

Objective. To investigate the IMRT treatment of nasopharyngeal carcinoma term effect, toxicity, and technical features. *Methods*. Sliding windows dynamic CT image-guided IMRT techniques on 31 patients for treatment of nasopharyngeal carcinoma radical radiotherapy, with 30 to 33 min irradiation. Target prescription dose GTVnx, GTVnd, CTV1, and CTV2 were 70~76Gy, 68~70Gy, 60~66Gy, and 54Gy, while giving a dose of vital organs, the brain stem, and other restrictions to protect the parotid gland. *Results*. During 3 to 18 months of follow-up for a median period of 10 months, 1-year locoregional patients' progression-free survival, distant metastasis-free survival, and overall survival rates were 93.5%, 87.1%, and 93.5%, respectively. Acute radiation reactions of grade I and II, xerostomia, and radioactive stomatitis were not observed. IMRT DVH analysis showed increased total dose and the irradiation target volume divided doses, reduced OARs illuminated, and the total dose divided doses. *Conclusion*. Intensity-modulated radiation therapy can achieve good short-term effects, significantly reduce the acute radiation response, and improve the quality of life of patients. It is worthy of promotion and application and in-depth research.

1. Introduction

Nasopharyngeal carcinoma is one of the common malignant tumors in China. Most patients can get radical and long-term survival after radiation therapy and chemotherapy. However, the sequelae of radiotherapy seriously affect the quality of life of some patients. How to further improve the efficacy of radiotherapy and reduce the sequelae is the interface of radiotherapy. Important challenges and issues: Intensity-modulated radiation therapy (IMRT) is an advanced radiotherapy technology that appeared at the end of the 20th century. It has the technical advantage of giving different doses to different areas at the same time to form a complex dose distribution. The application of IMRT in the treatment of nasopharyngeal cancer can improve the curative effect and reduce the sequela of radiotherapy. At the same time, it can improve the local control rate of nasopharyngeal cancer and improve the quality of life of patients. Our hospital launched image-guided IMRT in the treatment of nasopharyngeal carcinoma in November 2006 with good short-term effects. The results are reported below [1].

2. Wolf Swarm Algorithm

The harsh living environment and thousands of years of evolution have created a rigorous organization system for wolves and their sophisticated cooperative hunting methods. From the "wolf pack warfare" of the Mongolian iron rider during the Genghis Khan period to the "wolf pack submarine tactics" of Nazi German general Dunnitz to the electronic countermeasure weapon-"wolf pack attack system" researched by the US military, all highlight the wolf. The great charm of group wisdom: Wolves live in groups and have a clear social division of labor [2]. They unite and cooperate to bear their respective responsibilities for the survival and development of wolves. The algorithm uses a bottom-up design method based on the artificial wolf subject and a collaborative search path structure based on the

division of responsibilities. As shown in Figure 1, the whole process of wolf hunting is finally realized through the detection of prey scent and environmental information by individual wolves, the sharing and interaction of information between artificial wolves, and the individual behavior decisions of artificial wolves based on their own duties [3].

2.1. Migration Behavior. The solution space in addition to the best match SNUM wolf considered artificial probe wolf prey search in the solution space, and SNUM randomly selected an integer between $[n/(\alpha+1), n/\alpha]$, where α is the probe scaling factor wolves [4].

$$x_{\mathrm{id}}^{p} = x_{\mathrm{id}} + \sin\left(2\pi \times \frac{p}{h}\right) \times \mathrm{step}_{a}^{d}. \tag{1}$$

In this case, the probe wolf perceives odor concentration prey Y_{ip}, the prey with the highest odor concentration is selected and further updated to explore Wolf status X_i in the direction Y_{i0} with higher odor concentration; the above-mentioned process is repeated until a matching migration behavior sensing probe wolf prey to walk or odor concentration $Y_i > Y_{\mathrm{lead}}$ reaches the maximum number of times walk $T_{\max}$.

2.2. Summoning Behavior. Wolf howling initiated by summoning behavior convened horses around the fierce wolf to quickly move closer to the position where the wolf is, which is given by MNUM = n-SNUM-1; the howling of wolves is fierce with a relatively large step size $step_b$ quick raid approaching the position where the wolf is. During the wolf Meng i $k+1$-th iteration, the position is located at the d-dimensional space for the variable [5].

$$x_{\mathrm{id}}^{k+1} = x_{\mathrm{id}}^{k} + \mathrm{step}_{b}^{d} \cdot \frac{\left(g_{d}^{k} - x_{\mathrm{id}}^{k}\right)}{\left|g_{d}^{k} - x_{\mathrm{id}}^{k}\right|}, \tag{2}$$

where g_d^k is the position of the k-th generation wolf population in the d-dimensional space. Formula (2) consists of two parts, the former is the current position of the artificial wolf, and hunting reflects the basic wolf; wolf doing the latter represents a position with gradual wolf tendency to aggregate, to reflect the command wolf wolves. Raid way, if the fierce wolf prey i perceived odor concentration $Y_i > Y_{\mathrm{lead}}$, then $Y_i = Y_{\mathrm{lead}}$, the conversion of the wolf Meng wolf behavior and initiates call; if $Y_i < Y_{\mathrm{lead}}$, the fierce raid continues until i wolf head distance d_{is} between the s to join the ranks of attacks on prey is transferred to the siege of behavior is less than d_{near}. Optimization is provided to be in the range of variables d $[\min_d, \max_d]$, and it is determined that the distance d_{near} may be estimated from the following formula:

$$d_{\mathrm{near}} = \frac{1}{D \cdot \omega} \cdot \sum_{d=1}^{D} \left|\max_d - \min_d\right|, \tag{3}$$

where ω is distance determination factor that will affect the different values of the convergence rate of the algorithm and ω general increase will accelerate the convergence. However, ω wolf activity value is so high that it is beyond the wolf pack's hunting range, making it difficult for the prey to enter the circle, and the prey may escape or disappear [6].

2.3. Siege. Before the hunt is over, there is a wave of violent wolves assault. The wolves explore and besiege their prey together. The head wolf guards the place with the most prey. Specifically, for the k-th-generation wolves, prey provided at the position of the d-dimensional space is G_d^k, and wolves siege available behavior is given as follows:

$$x_{\mathrm{id}}^{k+1} = x_{\mathrm{id}}^{k} + \lambda \cdot \mathrm{step}_{c}^{d} \cdot \left|G_{d}^{k} - x_{\mathrm{id}}^{k}\right|, \tag{4}$$

wher λ is a random number [−1, 1] among uniformly distributed; step_c is performed when the artificial wolf i siege attacks on step. Artificial prey wolf perceived odor concentration greater than its original position after the state perceived behavior during the implementation of the siege of prey odor concentration; this location is updated manually wolf, and if not, the artificial wolf stays in the same position.

$$\mathrm{step}_{a}^{d} = \frac{\mathrm{step}_{b}^{d}}{2} = 2 \cdot \mathrm{step}_{c}^{d} = \frac{\left|\max_d - \min_d\right|}{S}, \tag{5}$$

where S is the step factor representing the degree of artificial wolf fine search of the optimal solution in the solution space. Figure 2 shows the basic steps of an intelligent algorithm, the wolf pack algorithm.

3. Materials and Methods

3.1. Clinical Data. 31 cases confirmed by pathological tissue with primary NPC from November 2018–December 2019 were selected, including 24 males and 7 females; aged 27 to 74 years, median age 47 years; and KPS score ≥80 minute. Pathology is PDSCC. Two cases were of Press 1992 Fuzhou staging I, 15 cases were of II period , 9 patients were of III, and 5 cases were of IV A (see Table 1). The study had been approved by the Medical Ethics Committee of Hospital, and the patients and their families had understood the situation of the study and signed the informed consent forms.

3.2. Treatment Methods

3.2.1. Radon Therapy. We used radical curative IMRT treatment. The patient was supine, and the head and neck were fixed with a thermoplastic mask. The CT simulation was performed with Siemens Plus4. The scanning range was from the top of the head to 1 cm below the clavicle head. All the scans were enhanced with a layer thickness of 3 mm or 5 mm and continuous scanning. The treatment planning system is Varian Eclipse version 6.5. The target area is defined according to the definitions of ICRU50 and 62 reports, and it is determined by referring to domestic and foreign literature reports. The gross tumor volume of the nasopharynx (GTVnx) (as shown in Figure 3) and the metastatic lymph nodes (GTVnd) of the neck (as shown in Figure 4) were delineated according to the boundaries of the lesions

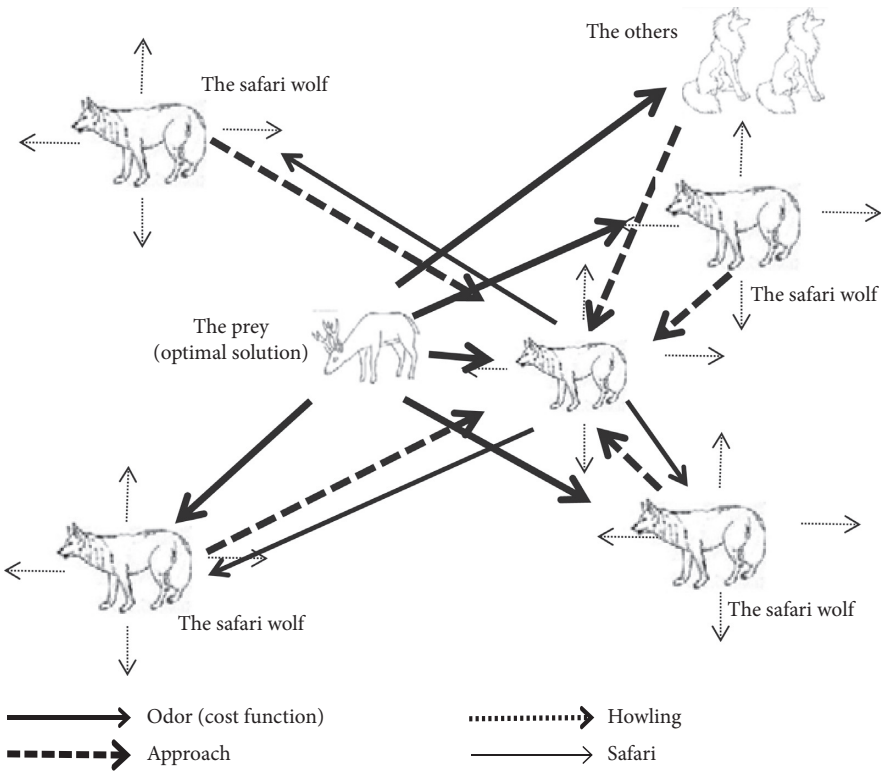

Figure 1: Decision chart of the wolf pack algorithm.

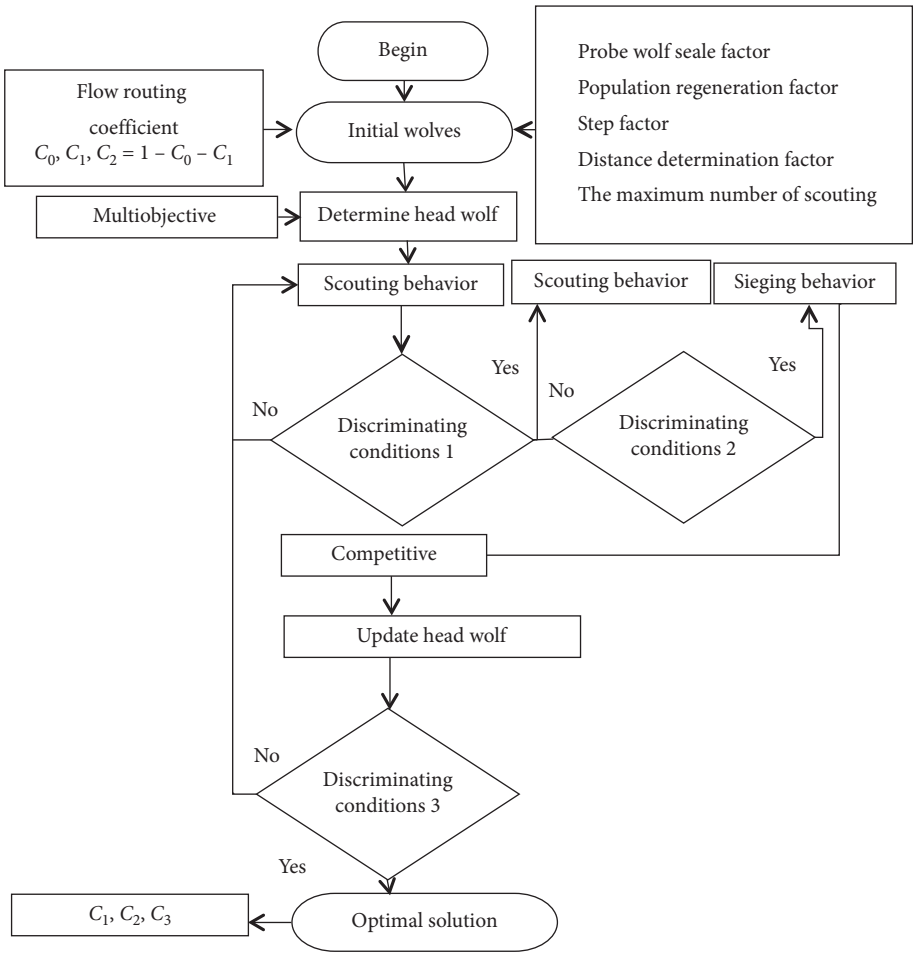

Figure 2: Basic steps of the wolf pack algorithm.

Table 1: *T* and *N* staging of 31 patients with nasopharyngeal carcinoma.

Staging	*T*1	*T*2	*T*3	*T*4	Total
*N*0	2	2	3	3	10
N	7	6	0	1	14
*N*2	1	4	1	0	6
N	0	1	0	0	1
Total	10	13	4	4	31

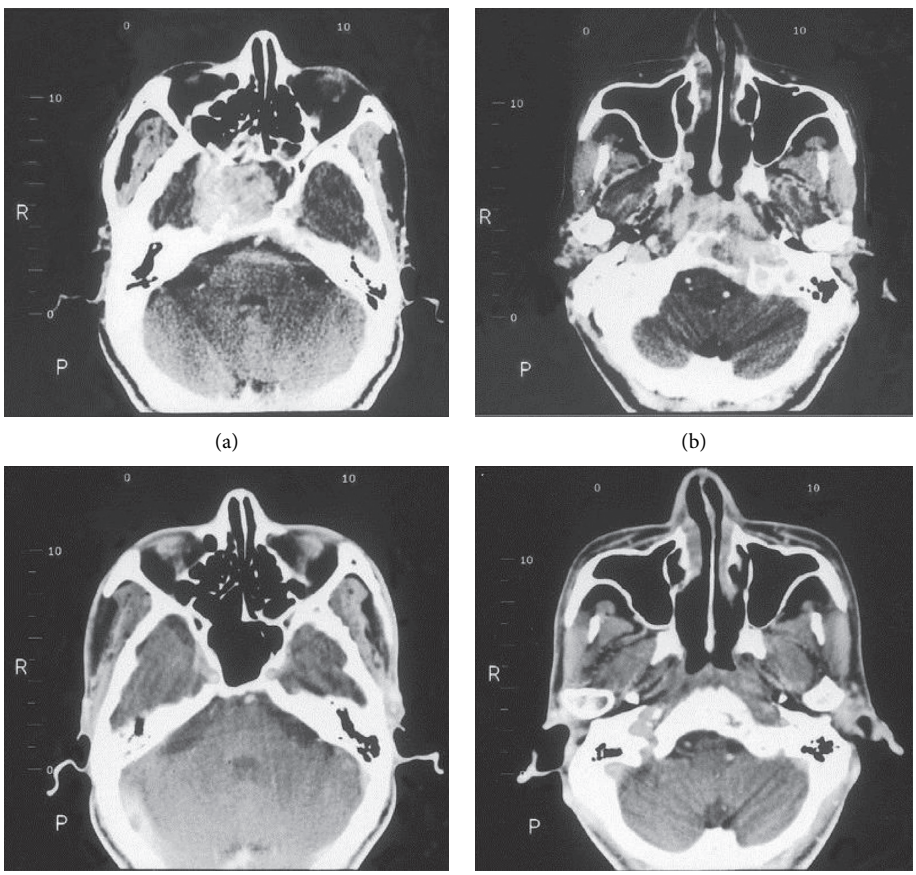

(a) (b)

(c) (d)

Figure 3: Nasopharyngeal gross tumor CT.

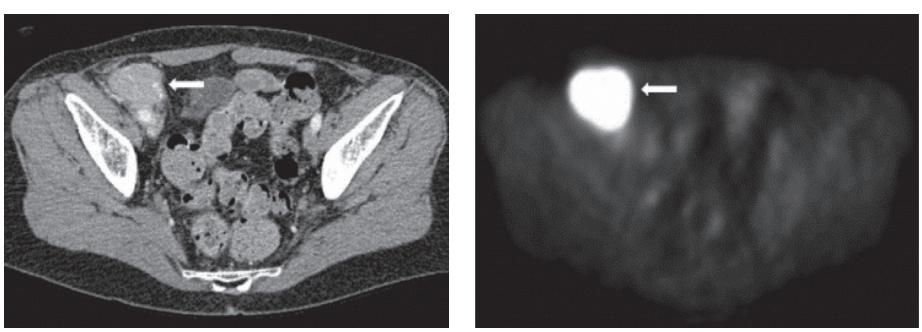

(a) (b)

Figure 4: Continued.

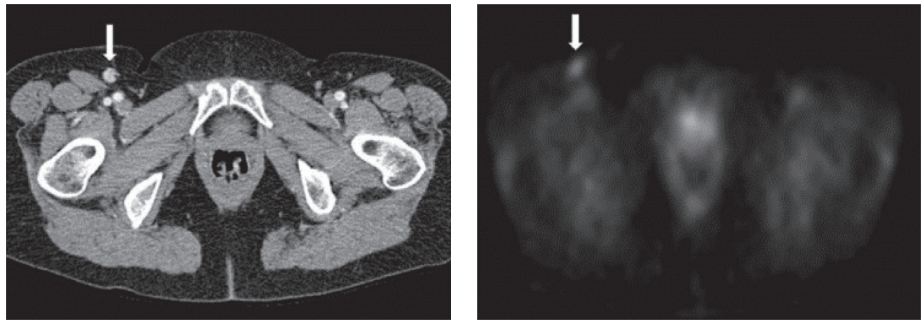

(c) (d)

Figure 4: CT of cervical metastatic lymph node tumors.

displayed by CT. Some cases were determined by referring to MRI or PET-CT images. The clinical target volume 1 (CTV1) is a high-risk area around the GTV. It is delineated according to the most likely orientation of the GTV and anatomical tumor invasion and lymphatic drainage. Its range is generally from the anterior boundary to the posterior wall of the maxillary sinus and the posterior boundary to the anterior vertebrae. The two sides include the parapharyngeal space, the upper boundary reaches the base of the skull, and the lower boundary reaches the level of the hyoid bone [7]. Clinical target volume 2 (CTV2) is the lymph node drainage area outside GTV that needs to be prevented from irradiation. The PTV is automatically generated by adding 3 to 5 mm to the target volume. Adjacent endangered organs mainly outline the brainstem, spinal cord, eyeball, and pituitary and parotid gland.

Target volume prescription doses of GTVnx, GTVnd, CTV1, and CTV2 were 70–76Gy, 68–70Gy, 60–66Gy, and 54Gy, respectively, and were irradiated 30–33 times. The organ-endangered dose was set as follows: brain stem ≤50Gy, spinal cord ≤40–45Gy, pituitary ≤30–50Gy, eyeball ≤5Gy, and parotid 50% volume ≤30Gy. The Eclipse6.5 planning system sliding windows dynamic intensity modulation mode was used for calculation and optimization. Nine field irradiations were used, and the irradiation angles were 320, 280, 240, 200, 160, 120, 80, 40, and 0 degrees. After the calculation was completed, the target volume and the organ-endangered dose distribution were evaluated based on DVH and on the CT image level. A map treatment system was used to verify the treatment plan before treatment [8].

Varian 23EX image-guided linear accelerator 6MV-X irradiation was used for the treatment. The patients were given cone beam CT scans before the first 3 treatments, and some patients were scanned once a week during subsequent treatments to ensure positioning and repetition. The accuracy of the treatment is described in previous reports.

3.2.2. Chemotherapy. Of the 31 patients, 24 were treated with radiochemotherapy. Among them, 21 patients received 1 to 2 induction chemotherapies before radiotherapy, and 19 patients received 1 to 5 adjuvant chemotherapies after radiotherapy. PF was used for chemotherapy: cisplatin 60–80 mg/m^2, intravenous infusion on the first day, fluorouracil 500–750 mg/m^2, and intravenous infusion on the 1st to 5th day. This was repeated at 3-week intervals.

3.3. Observation and Follow-Up. We observed and recorded acute reactions during treatment. After treatment, every 3 to 6 months, a second conventional CT review of the nasopharynx and blood, B ultrasonic chest and abdomen, abdominal CT, or isotopic bone scan were performed if necessary. Acute reaction was evaluated according to RTOG criteria. Follow-up time from the start to end of radiotherapy: median follow-up of 10 months' (from 3 to 18 months) follow-up was 100%.

3.4. Statistical Analysis. We used the Kaplan–Meier method for calculating overall survival, progression-free survival, and local area without distant metastases.

4. Result

4.1. Clinical Efficacy. After the treatment, 3 months or 6 months later, there were 3 cases of CT nasopharyngeal residual primary tumor , 2 cases of cervical lymph node residue and nasopharyngeal primary tumor, and a cervical lymph node metastasis regression rate of 90.6% and 93.8%, respectively, was observed. During the follow-up, nasopharyngeal primary tumor recurrence or cervical lymph nodes were not observed. Four cases of distant metastasis were observed, with two cases of bone metastasis, one case of lung metastasis, and 1 case of multiple parts of the transfer, and the transfer time of occurrence after radiotherapy was 3 to 16 months; 2 died, one case by 5 months after radiotherapy nasopharyngeal massive hemorrhage death and 1 three months after radiotherapy due to coinfection with multiple distant metastases failure and death. Patient 1-year locoregional progression-free survival, distant metastasis-free survival, and overall survival rates were 93.5%, 87.1%, and 93.5%, respectively.

4.2. Acute Radiation Reaction. According to the US acute radiation reaction Radiation Therapy Oncology Group (RTOG), acute radiation reaction score appears at the end of evaluable patients treated. There was incidence of acute skin

radiation, oral and oropharyngeal mucosa, dry mouth, and bone marrow suppression in this group of patients. The patients were able to tolerate the radiation reaction after symptomatic treatment, which did not affect the normal progress of radiation therapy (see Table 2).

4.3. Dose Distribution and Dose Volume Histogram Analysis. The IMRT dose distribution was irradiated at different prescribed doses in different target areas, while important organs such as the parotid gland and brainstem were only exposed to low doses, thereby being protected. The maximum, minimum, and average exposure doses of different target volumes show that the target area has a more uniform dose distribution, avoiding the occurrence of severe cold spots and hot spots. The single dose of GTV is significantly higher than that of conventional irradiation, and the average fractional dose is 2.26–2.35Gy, while the single dose of CTV is the same as that of conventional irradiation, 1.75–2.018Gy. The exposure doses of endangered organs in this group all met the prescribed dose requirements, and they were all within their tolerable dose range (see Table 3 and Figure 5).

Table 2: 31 cases of acute radiation reaction after IMRT in 31 patients with nasopharyngeal carcinoma (cases).

Adverse reactions	Toxicity classification				
	0	I	II	III	IV
Skin reaction	0	12	10	9	0
Mucosal reaction	0	6	15	10	0
Dry mouth	0	10	13	8	0
Myelosuppression	24	4	2	1	0

Table 3: 31 patients with nasopharyngeal carcinoma who received IMRT target volume irradiation dose (Gy).

Target volume	GTVnx	GTVnd	CTV1	CTV2
Mean maximum dose	78.02	75.24	76.45	67.59
Minimum dose means	70.48	67.15	49.45	45.84
Average measurement average	75.2	71.3	68.78	58.95
Mean fractional dose	2.35	2.26	2.18	1.75

5. Discussion

The radiotherapy efficacy of nasopharyngeal carcinoma is closely related to the radiation dose, tumor volume, and uniformity of dose distribution in the target area [9, 10]. Nasopharyngeal carcinoma is a dose-related tumor. In a certain range, the local control rate of the tumor is positively correlated with the radiation dose. Therefore, people have tried different techniques to improve its therapeutic effect. The conventional two-dimensional radiotherapy method is limited by the tolerance dose of the surrounding sensitive organs. It is impossible to increase the radiation dose to improve the efficacy and reduce the sequelae. On the basis of conventional radiotherapy, intracavitary radiotherapy or three-dimensional stereotactic radiotherapy to increase the radiation dose of primary nasopharyngeal lesions can increase the local radiation dose to a certain extent, but the radiation response and sequelae caused by conventional radiotherapy cannot be alleviated. IMRT can irradiate different target areas with different doses at the same time, which can form a highly complex-shaped dose distribution. Its dosimetry characteristics have significant advantages over conventional radiotherapy and three-dimensional conformal radiotherapy, especially meeting the requirements for the treatment of nasopharyngeal cancer. It has the potential to further improve the efficacy of nasopharyngeal cancer and reduce the acute and long-term reactions of radiation therapy.

The recent treatment results of 31 patients in this group are encouraging. The primary nasopharyngeal focus and cervical metastatic lymph node regression rates were 90.6% and 93.8% 3 to 6 months after treatment, although compared with the work of Zhao Chong et al. The 6-month nasopharyngeal primary lesions and cervical metastatic lymph node regression rates were 96.4% and 98.6%, respectively. The results were slightly lower, but some patients were observed earlier, and some lesions were expected to recede with time. No recurrence of primary nasopharyngeal lesions and recurrence of cervical lymph nodes were observed in this group during follow-up. The 1-year local area progression-free survival rate, distant metastasis-free survival rate, and overall survival rate were 93.5%, 87.1%, and 93.5%, respectively. It is suggested that IMRT can obtain satisfactory local and regional control in newly treated nasopharyngeal carcinoma cases. The results of this group are comparable to the advanced level reported in other studies. The important advantage of IMRT treatment for nasopharyngeal carcinoma is reflected in reducing the radiation dose of important organs and normal tissues, thereby reducing the acute phase response and sequelae of treatment. In this group of 31 cases, 70% of patients had grade 0 to 2 acute reactions, 30% of patients had grade 3 acute reactions, and no grade 4 acute reactions appeared. All patients completed treatment on time. It was reported that 67 patients with nasopharyngeal carcinoma treated with IMRT were treated with 76% of patients with only grade 1 or 2 side effects, 22% had grade 3 side effects, and only 1 case had grade 4 reactions. The grade 3 acute response of this group of patients is slightly higher than that in the work of Lee et al., which may be related to our caution in the initial stage of IMRT and the conservativeness of the CTV target area. With the accumulation of treatment experience, we have improved the outline of the target area CTV1. At present, we have observed changes in the reduction of the acute response. Most patients in this group showed a grade 0 to 2 dry mouth acute response after IMRT treatment, and during the follow-up period, the dry mouth symptoms of the patients gradually reduced over time, which were significantly milder those that of patients receiving conventional radiotherapy, showing theadvantages of IMRT treatment on salivary gland function.

One patient in this group died of nasopharyngeal hemorrhage 5 months after treatment. The patient's local lesion was T3, and the irradiation dose was 76Gy/30 times, which was completed in 6 weeks. The occurrence of major bleeding in this patient may be related to the high dose of a

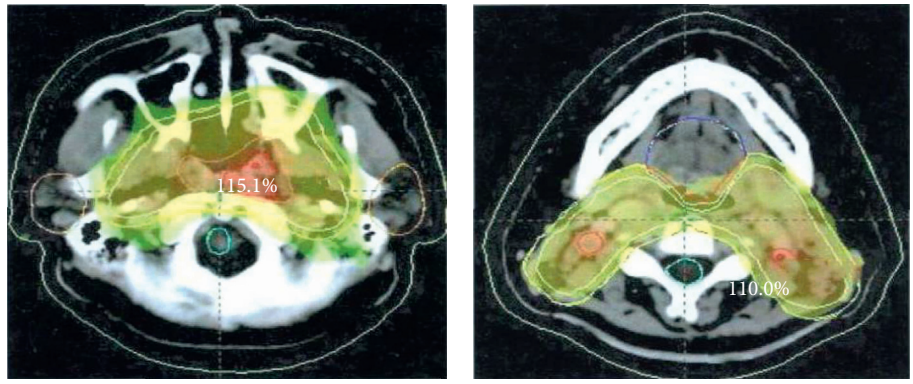

(a) (b)

Figure 5: IMRT dose distribution.

single irradiation. Although there is only one case of major bleeding, it should also be given high attention.

The IMRT treatment in this group uses image-guided technology to ensure highly accurate positioning errors and repeatability of treatment. It is important to ensure the treatment effect and reduce the exposure to organs. Strong technical support is needed for implementation.

6. Conclusions

In short, IMRT can be used to treat nasopharyngeal carcinoma with satisfactory short-term effects. The acute radiotherapy response can be tolerated, and it has a good protection effect on important organs such as the parotid gland

Data Availability

No data were used to support this study.

Conflicts of Interest

The authors declare that they have no conflicts of interest.

Acknowledgments

This work was supported by the General Project of the Hainan Natural Science Foundation (No. 818MS152).

References

[1] S. B. Liang, J. J. Teng, and X. F Hu, "Prognostic value of total tumor volume in patients with nasopharyngeal carcinoma treated with intensity-modulated radiotherapy," *BMC Cancer*, vol. 17, no. 1, p. 506, 2017.

[2] Y.-H. Lin, T.-L. Huang, C.-Y. Chien et al., "Pretreatment prognostic factors of survival and late toxicities for patients with nasopharyngeal carcinoma treated by simultaneous integrated boost intensity-modulated radiotherapy," *Radiation Oncology*, vol. 13, no. 1, p. 45, 2018.

[3] Y.-H. Young, "Irradiated ears in nasopharyngeal carcinoma survivors: a review," *The Laryngoscope*, vol. 129, no. 3, pp. 637–642, 2019.

[4] M. Y. Wu, X. Y. He, and C. S. Hu, "Tumor regression and patterns of distant metastasis of t1-t2 nasopharyngeal carcinoma with intensity-modulated radiotherapy," *Plos One*, vol. 11, no. 4, Article ID e0154501, 2016.

[5] Wu Xin, H. Jingwen, L. Lei, Li Hongmei, and X. Li, "Cetuximab concurrent with imrt versus cisplatin concurrent with imrt in locally advanced nasopharyngeal carcinoma: a retrospective matched case-control study," *Medicine*, vol. 95, no. 39, Article ID e4926, 2016.

[6] F. Liu, T. Jin, L. Liu, Z. Xiang, R. Yan, and H Yang, "The role of concurrent chemotherapy for stage ii nasopharyngeal carcinoma in the intensity-modulated radiotherapy era: a systematic review and meta-analysis," *Plos One*, vol. 13, no. 3, Article ID e0194733, 2018.

[7] V. H. Lee, D. L. Kwong, and T. W Leung, "Prognostication of serial post-intensity-modulated radiation therapy undetectable plasma ebv dna for nasopharyngeal carcinoma," *Oncotarget*, vol. 8, no. 3, 5308 pages, Article ID 5292, 2017.

[8] Xu Peng, M. Yanmei, B. Pierre, F. Mei, and L. Jinyi, "Incidence of small lymph node metastases in patients with nasopharyngeal carcinoma: clinical implications for prognosis and treatment," *Head & Neck*, vol. 39, no. 2, Article ID 305, 2016.

[9] W. Zhao, H. Lei, and X Zhu, "The clinical characteristics of secondary primary tumors in patients with nasopharyngeal carcinoma after intensity-modulated radiotherapy: a retrospective analysis," *Medicine*, vol. 95, no. 45, Article ID e5364, 2016.

[10] W. Z. Sun, D. D. Zhang, and Y. L Peng, "Retrospective dosimetry study of intensity-modulated radiation therapy for nasopharyngeal carcinoma: measurement-guided dose reconstruction and analysis," *Radiation Oncology*, vol. 13, no. 1, Article ID 42, 2018.